Measurements and Simulations of Impedance Reduction Techniques in Particle Accelerators

A thesis submitted to the University of Manchester for the degree of

Doctor of Philosophy

in the Faculty of Engineering and Physical Sciences

2011

Hugo Alistair Day

School of Physics and Astronomy

Contents

Total word count: 27794

List of Tables

List of Figures

Abstract

A review of the first two years of study are presented. These topics consist of; Simulations of coaxial wire measurements of the impedance of asymmetric devices, coaxial wire measurements of ferrite kicker magnets for use in the SPS and LHC and impedance studies of a number of potential collimator upgrades for the LHC, focusing on the phase 2 secondary collimators for the LHC. Also disucssed is future work towards completion of the PhD and a timetable of writing to ensure timely completion.

Declaration

No portion of the work referred to in this thesis has been submitted in support of an application for another degree or qualification of this or any other university or other institution of learning.

Hugo Alistair Day

School of Physics and Astronomy

University of Manchester

Oxford Road

Manchester

M13 9PL

November 2006

Copyright

Contents

Chapter 1

Introduction

Chapter 2

Wakefields and Impedance

2.1 Wakefields, Impedances and Beam Dynamics Effects

2.2 Theoretical Background of Wakefields and Impedances

- Wakes
  - Introduction to the electromagnetic field of charged particle moving in free space
  - Field of a particle in a perfectly conducting pipe - method of image currents
  - Place a witness particle distance s behind source particle and deduce electric field as seen by this particle
  - normalise this by the source particle charge to give the wakepotential
  - And again by the source particle charge and current profile to acquire the loss factor
  - Longitudinal field predominantly
  - Introduce the Panowsky-Wenzel theorem covering transverse field - Transverse wakes
- Impedance

- Firstly mention the commonality of frequency dependent material properties - ferrite permeability, permitivitty determined by conductivity/frequency in conductors/dielectrics/skin depth
- Fourier transform of wakefield into the convolution of the beam current spectrum and the impedance
- Again Panowsky-Wenzel for impedance
- Discussion of the transverse impedance - in particular the general definition of an impedance (n-th order current interacting with an m-th order field)
- Define dipolar/driving and quadrupolar/detuning impedance. In addition constant transverse impedance term

2.2.1 Resistive Wall Impedance

- Return to simple axisymmetric geometry concerning a finite conductivity of the wall
- Derive in frequency domain - then have impedance. Give an example wakefield of a good conductor (copper), bad conductor (graphite), non-conductor (ferrite)

2.2.2 Geometric Impedance

Derive the field pattern for a pillbox cavity - Oscillating fields with a characteristic frequency of some multiple of the lowest eigenfrequency

2.3 Examples of Effects

2.3.1 Beam Induced Heating

One consequence of the presence of longitudinal impedance is the phenomena of beam-induced heating. First we should consider the so called parasitic loss of a charged particle interacting with a generic impedance[ref Chao/Ng];

$$\Delta E = -2\pi e^2 N_b \int_{-\infty}^{\infty} d\omega \left|\lambda\left(\omega\right)\right|^2 Z_{\parallel}\left(\omega\right) \tag{2.1}$$

where ΔE is the energy loss per pass per particle, e is the charge per particle, N_b, ω the frequency, λ the line density of the bunch and $Z_{\parallel}$ the longitudinal impedance of the object being traversed.

Due to the decay of the wakefields induced by this energy loss, this energy must eventually be lost to the device causing the impedance (valid below the cutoff frequency of the machine beam pipe). Therefore we can assume that the energy loss from the particles is absorbed by the surrounding structure. Summing over all particles in a bunch we can therefore obtain a sum of the energy loss;

$$\Delta E_{bunch} = 2\pi \left(eN_b\right)^2 \int_{-\infty}^{\infty} d\omega \left|\lambda\left(\omega\right)\right|^2 Z_{\parallel}\left(\omega\right) \tag{2.2}$$

As often we must deal with machines storing multiple bunches, for these we simply multiply the energy loss per bunch by the number of stored bunches;

$$\Delta E_{buunches} = 2\pi \left(eN_b\right)^2 n_{bunch} \int_{-\infty}^{\infty} d\omega \left|\lambda\left(\omega\right)\right|^2 Z_{\parallel}\left(\omega\right) \tag{2.3}$$

where n_{bunch} is the number of bunches in the machine. If we assume a revolution frequency f_{rev} we thus get a power loss of;

$$\begin{aligned}
P_{loss} =& \Delta E_{bunches} f_{rev} \\
=& 2\pi f_{rev} \left(eN_b\right)^2 n_{bunch} \int_{-\infty}^{\infty} d\omega \left|\lambda\left(\omega\right)\right|^2 Z_{\parallel}\left(\omega\right) \\
=& \omega_{rev} \left(eN_b\right)^2 n_{bunch} \int_{-\infty}^{\infty} d\omega \left|\lambda\left(\omega\right)\right|^2 Z_{\parallel}\left(\omega\right) \\
=& \omega_{rev} \left(eN_b\right)^2 n_{bunch} \int_{-\infty}^{\infty} d\omega \left|\lambda\left(\omega\right)\right|^2 \left(\Re e\left(Z_{\parallel}\left(\omega\right) + \Im m Z_{\parallel}\left(\omega\right)\right)\right).
\end{aligned} \tag{2.4}$$

As $\Re e\left(Z_{\parallel}\left(\omega\right)\right)$ is an even function and $\Im m\left(Z_{\parallel}\left(\omega\right)\right)$ is an odd function, we see that

$$P_{loss} = \omega_{rev} \left(eN_b\right)^2 n_{bunch} \int_{0}^{\infty} 2d\omega \left|\lambda\left(\omega\right)\right|^2 \Re e\left(Z_{\parallel}\left(\omega\right)\right). \tag{2.5}$$

Next we make a change of the variable of integration $\omega = nbunch\omega_{rev}$;

$$P_{loss} = \omega_{rev} \left(eN_b\right)^2 n_{bunch}^2 \int_0^\infty 2d\omega_{rev} \left|\lambda \left(\omega_{rev} n_{bunch}\right)\right|^2 \Re e \left(Z_{\parallel} \left(\omega_{rev} n_{bunch}\right)\right). \quad (2.6)$$

We can subsequently change to a sum formalism to obtain

$$P_{loss} = \left(\omega_{rev} eN_b n_{bunch}\right)^2 \sum_{n=0}^{\infty} \left(2 \left|\lambda \left(\omega_{rev} n_{bunch}\right)\right|^2 \Re e \left(Z_{\parallel} \left(\omega_{rev} n_{bunch}\right)\right)\right) \quad (2.7)$$

$$P_{loss} = \left(\omega_{rev} eN_b n_{bunch}\right)^2 \sum_{n=0}^{\infty} \left(2 \left|\lambda \left(\omega_0\right)\right|^2 \Re e \left(Z_{\parallel} \left(\omega_0\right)\right)\right) \quad (2.8)$$

where $\omega_0 = 2\pi f_0$, $f_0 = \frac{1}{\tau_b}$ and τ_b is the bunch spacing.

Often we define the impedance of a structure using a resonator model, where the impedance is defined as

$$Z_{\parallel} \left(\omega\right) = \frac{R_s}{1 + Q\left(\frac{\omega_{res}}{\omega} - \frac{\omega}{\omega_{res}}\right)} \quad (2.9)$$

where R_s is the shunt impedance, Q the quality factor, ω the frequency and ω_{res} the resonant frequency

It is often useful to make the distinction between heating due to a broadband impedance (interacts with many spectral lines) and a narrowband impedance (interacts with only one spectral line). This is due to the different ways in which the heating due to these impedances changes with increasing or decreasing the number of bunches in a machine.

Heating Due to a Broadband Impedance

For a broadband impedance (i.e. $Q < 100$) we can evaluate the sum above as either a sum or an integral. There are some key points to note for this regime of beam-induced heating. Firstly, the power loss due to a broadband impedance increases linearly with the number of bunches $n_{bunches}$. This is due to the number of spectral lines that the impedance interacts with (illustrated in Fig. **??**) being inversely proportional to the bunch spacing, which is typically proportionall to the number of bunches in a storage ring.

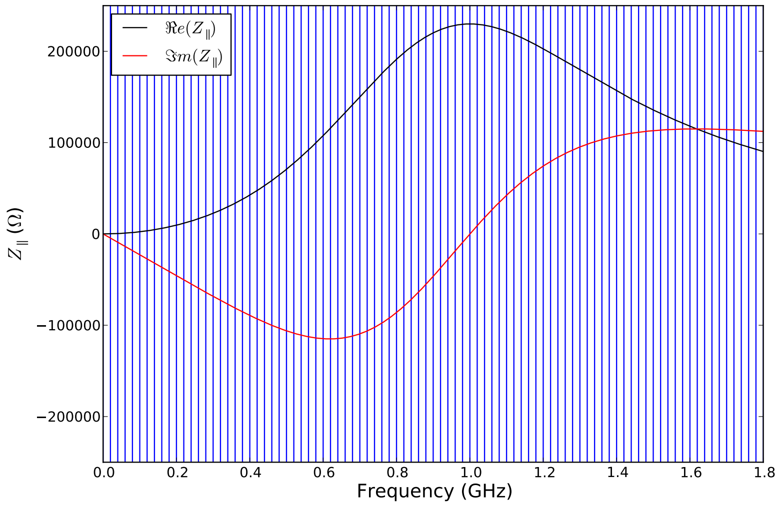

(a)

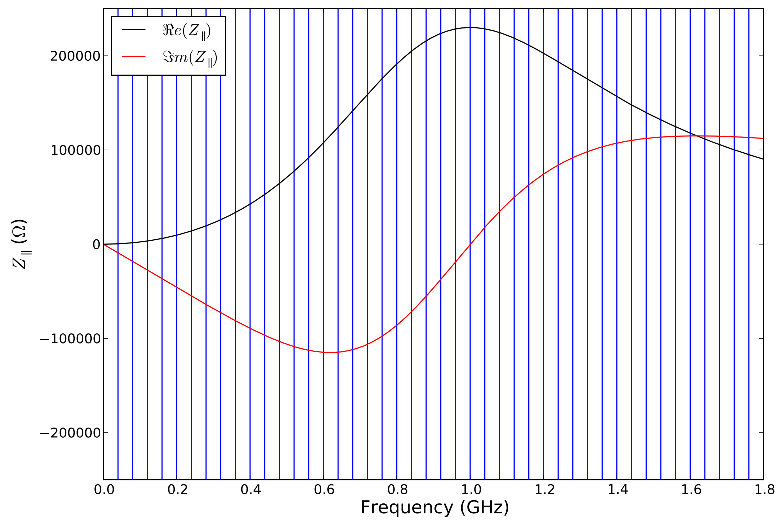

(b)

Figure 2.1: The spectral lines of a beam with **??** 50ns bunch spacing and **??** 25ns bunch spacing with a broadband impedance ($R_s = 0.23M\Omega, Q = 1, \omega_0 = 1$GHz)

Figure 2.2: The change in power loss due to a broadband impedance with an increased number of bunches in a storage ring

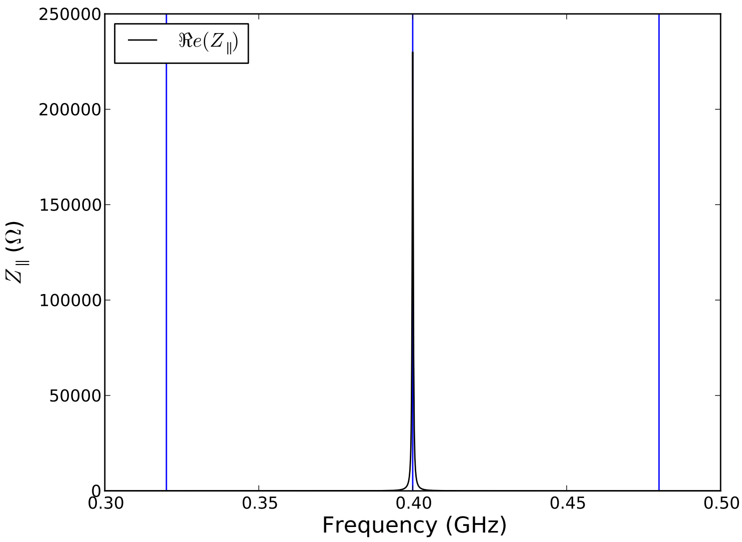

Figure 2.3: The spectral lines overlaying on a narrow band impedance. The spectral lines (in blue) are for $\omega_0 = 40$MHz. Note how only a single spectral line lies on this impedance.

Note that technically the increase is linear with number of bunches due to the increase seperation of spectral lines

Heating due to a Narrowband Impedance

For narrow band impedances (Q≫100) which lie upon a single spectral line (i.e. $\omega_{res} = mn_{bunch}\omega_0$, where m is some integer) we can see that the power loss due to this spectral line becomes from Eqn. **??**

$$P_{loss} = (\omega_{rev} e N_b n_{bunch})^2 \left(2\left|\lambda\left(\omega_{res}\right)\right|^2 \Re e\left(Z_\parallel\left(\omega_{res}\right)\right)\right) \tag{2.10}$$

It can thus be seen the power loss scales with n_{bunch}^2. And example of this can be seen in Table **??**

table

2.3.2 Single Bunch and Coupled Bunch Instabilities

- Take references to introductory section on beam dynamics - longitudinal and transverse oscillations
- Introduce bunch oscillation spectra - resonance diagrams for transverse motion, longitudinal spectra
- Instabilities by resonance crossing, LMCI, TMCI, headtail instabilities, TCBI
- Section on landau damping/transverse dampers? Other way to counter large impedances.

2.3.3 Example of LMCI with Broadband and Space Charge Impedances Studied with HEADTAIL

Chapter 3

Bench Top Measurements of Beam Coupling Impedance

Chapter 4

Computational Simulations of Beam Coupling Impedance

4.1 Time Domain Simulations

- A VERY general introduction to time domain simulations codes. This is not a thesis of computational methods, only one thing you may do with them. Write this way
- General experience - advantages of time domain methods (speed, memory footprint). Weaknesses (mesh resolution of structure, CPU limitation, long simulations times for high-Q resonances)

4.1.1 Direct Simulation of a Particle Beam

- Introduction to time domain code - simulation of a generic time signal, and the integration path
- How we can subsequently simulate various types of impedance as a result
  - Longitudinal - At various displacements
  - Transverse - dipolar/quadrupolar/constant with displacements of either the signal or the integration path, and subsequently taking gradient of resulting

impedance

4.2 Frequency Domain Simulations

- Advantages of frequency domain - good resolution of structure by meshing, fast solution for individual modes, accurate for resonant structures. Weaknesses - Very memory intensive. Very time consuming to characterise structures over a large frequency ranges

4.2.1 Eigenmode Simulations

- To identify cavity modes of structures
- Extract the resonant frequency and Q of cavity modes
- fields on axis/off axis to extract R/Q, transverse R/Q

4.2.2 The Coaxial Wire Method by Simulation

- port solutions for driven modal simulations
- Allow the extraction of S21
- Evaluate as in previous section

4.2.3 Simulation of the particle beam

- Refer back to the nature of the EM field surrounding a charged particle beam (TEM-like)
- We can enforce a TEM like profile on emitted radiation of a surface
- With a TEM source with no wire - basically a particle beam
- Evaluation as mentioned in Oleksey's paper

Chapter 5

Beam Coupling Impedance Reduction Techniques

Chapter 6

Case Studies

6.1 LHC Injection Kicker Magnet

- Introduction to the kicker magnet system
    1. What are kicker magnets - Injection/Extractions systems
    2. Why are they potentially a problem
- Explain the background of the LHC-MKI in particular
    1. The original concern over heating, subsequent design of the beam screen
    2. Observed problems with electrical breakdown of the beam screen, and subsequent removal of screen conductors
    3. Recent observed heating in MKIs
- Summarise current state of the MKIs in the LHC - Beam screen layouts, two sets of kickers, one all of 15 screen conductors, one has one with 24
- Comparison of the measurements and simulations of the LHC-MKI
    1. Measurements of the Longitudinal BCI of the MKI - before and after bake out, with 15 and 19 screen conductors

2. Measurements of the transverse BCI of the MKI - if time just for interest and as a verification of the asymmetric method

- A breakdown of the impedance that we see in the MKI

  1. Start with a simple c - core ferrite magnet
  2. Add a ceramic tube
  3. Add screen conductors in internal side - Brief interlude about the limitations this places on the magnet rise time due to creating a Faraday cage
  4. Add the capacitive coupling - Different lengths of overlap to demonstrate that this controls the frequency of the resonances. Also lengths of the screen conductors for lower resonances
  5. Add the ferrite damping rings - damp resonances of length of screen conductor - not(!) overlap
  6. Hopefully show that this is the dominant cause of the resonances

- Summary of different beam screen designs - Where possible include discussion about the reduction of the voltage build up on each screen conductor

  1. Screen conductors all of the same length with capactive coupling at one end - Show how increasing the number of screen conductors really helps to reduce the BCI
  2. Screen conductors with a tapering of the length, with the longest at the side towards the ground plate and the shortest towards the HV plate
  3. Alternating lengths of long and short screen conductors
  4. Having the screen conductors in closed slots in the ceramic tube
  5. The addition of small conducting spheres to the ends of the screen conductors to reduce the high fields at the conductor ends
  6. Thicker ceramic at the capacitively coupled end of the beam screen to reduce the field gradient

7. Alternative beam screen design - Most screen conductor capactively coupled at both ends, with two connected to the beam pipe at one end. Aim to reduce the potential on all conductors by conductively connecting them at the capactively coupled end
8. Stepping the external metallization away from the ceramic tube at the ends of the screen conductors. The metallization will be removed and a conducting pipe placed there instead - different step out dstances are investigated

- Heating estimates for all of the above

1. Explain completely the methods of estimating the power losses here - bunch intensity, number of bunches, bunch length, distribution
2. Note the benefits of increasing the bunch length for the resonances with 15 screen conductors
3. Summary charts of the beam induced heating for the others, and plots illustrating how the changes in bunch length changes the power loss
4. Impedance profiles of all of the above - longitudinal predominantly
5. Some judgement on which is most appropriate for an impedance point of view
6. Comments on the improvements made to existing magnets already - 19 screen conductors

6.2 LHC Phase 2 Collimator Designs

- Introduction to the collimator upgrade project - Why are collimators important

1. The have two significant physical requirements - a rigid, sturdy material and must be placed very close to the beam
2. The first necessitated the use of graphite/carbon materials for the phase 1 collimators due to their survivability in the condition needed. The second means that the resistive wall impedance is very large

- Phase 2 collimator materials choice
  1. Why a phase 2 collimator upgrade?
  2. Summary of the material requirements and the available materials
  3. Simple model used - simulations and comparison to analytical models
- TCTP Impedance Studies
  1. What is the TCTP? Why do we need it?
  2. Possibly designs
     - Structure with RF fingers isolating the beam from the vacuum tank
     - Structure with a narrow connection between central cavity and vacuum tank - simulated with and without ferrite to demonstrate reduction in Q
  3. Simulations Parameters and results
  4. Heating estimates - using single bunch, multi-bunch, on resonance and equally spaced
  5. Localisation of the heating - using both CST and HFSS